

Incorporation of Cu-N_x cofactors into graphene encapsulated Co as biomimetic electrocatalysts for efficient oxygen reduction

Materials and Methods:

Materials synthesis:

Precursor of Cu₃[Co(CN)₆]₂ was synthesized according to following process:

Solution A: Cu(NO₃)₂·3H₂O (1.5 mmol, 362.4 mg) and trisodium citrate dehydrate surfactant (0.6 g) were dissolved in deionized H₂O (50 mL) under agitated stirring to obtain a transparent blue solution. Solution B: K₃[Co(CN)₆]₂ (332.4 mg, 1 mmol) was also dissolved in deionized water (50 mL). Solution A was slowly added to solution B to form a blue colloid solution. The whole reaction was performed at room temperature with agitated stirring. After 20 minutes, the reaction was aged for 24 h at room temperature without any interruption. The resulting blue-colored precipitate was filtered and washed several times with distilled water and finally dried in air at 60°C.

CuCo-600, CuCo-700 and CuCo-800 were obtained by directly carbonization of Cu₃[Co(CN)₆]₂ within N₂ atmosphere under different temperatures (600°C, 700°C, 800°C) with a heating rate of 5 °C min⁻¹ and kept for 2 h.

To obtain samples of S-600, S-700 and S-800, the as-annealed CuCo bimetal powders were further treated with excess of 0.1 M FeCl₃ overnight. The final product was then collected, washed with a copious amount of distilled water several times and finally dried in vacuum oven.

The Co-600 used as reference was obtained by directly carbonization of Co₃[Co(CN)₆]₂. The typical synthetic process of Co₃[Co(CN)₆]₂ was similar with Cu₃[Co(CN)₆]₂ except that Cu(NO₃)₂·3H₂O was replaced by Co(NO₃)₂·6H₂O.

To obtain samples of Co-600A, the as-annealed Co-600 powder was further treated with same etching process as for S-600.

The Cu/C and pure graphene used as reference was synthesized from Cu-btc precursor and with a

modified Hummers' method, respectively according to previous study.(33,36)

Material characterization:

The powder XRD patterns of the samples were recorded with an X-ray diffractometer (Japan Rigaku D/MAX- γ A) using Cu-K α radiation ($\lambda=1.54178$ Å) with 2θ range of 20–80°. FESEM images were taken on a JEOL JSM-6700M scanning electron microscope. TEM images were collected from Hitachi H-800 transmission electron microscope using an accelerating voltage of 200 kV, and a HRTEM (JEOL-2011) was operated at an accelerating voltage of 200 kV. TGA was carried out using a Shimadzu-50 thermoanalyser under flowing nitrogen atmosphere and with a heating rate of 10°Cmin⁻¹. XPS was performed on an ESCALAB 250 X-ray photoelectron spectrometer using Al K α radiation. Inductively coupled plasma atomic emission spectroscopy (ICP-AES) was carried out in Optima 7300 DV. The samples for ICP analysis were first heated at 800 °C for 4 h in air, followed by treatment in concentrated chloroazotic acid for several hours until the material was fully dissolved. The specific surface area was evaluated at 77 K (Micromeritics ASAP 2020) using the Brunauer–Emmett–Teller (BET) method applied to the adsorption branch. The X-ray absorption near edge structure (XANES) and the extended X-ray absorption fine structure (EXAFS) were investigated at the BL08U1A and BL14W1 beamlines of Shanghai Synchrotron Radiation Facility (SSRF). All the samples were characterized using Cu-K edge XANES and EXAFS in a transmission mode under ambient conditions. Cu L-edge and N K-edge XANES spectra were measured at the beamline BL08U1A in the total electron yield (TEY) mode by collecting the sample drain current under a vacuum better than 10⁻⁷ Pa. The absorption spectra of Cu K-edge were collected in transmission mode using a Si (111) double-crystal monochromator at BL14W1 beamline. The data was normalized and analyzed using Athena and Artemis software. The background subtraction and normalization procedures were carried out using standard routines with default parameters determined by the Athena software.

Calculation details:

We perform DFT calculations using the Vienna Ab Initio Simulation Package (VASP), the generalized gradient approximation (GGA) of Perdew–Becke–Ernzerhof (PBE) is used for the exchange-correlation functional. The cut-off energies for plane waves is 400 eV, providing a

convergence of 10^{-5} eV in total energy and 0.02 eV/Å in Hellmann Feynman force on each atom. A Monkhorst-Pack $3 \times 3 \times 3$ k-point grid was used to sample the Brillouin zone for structure optimization and $9 \times 9 \times 9$ k-point grid was used for DOS calculation. The free energies of the intermediates at 298.15 K were obtained using $\Delta G = \Delta E + \Delta ZPE - T\Delta S + eU$ according to previous work (36,49), where ΔE is the binding energy of adsorption species HO*, O* and HOO*, ΔZPE , ΔS and U are the zero point energy changes, entropy changes and applied potentials, respectively.

Electrochemical Measurements:

The electrochemical tests were carried out in a three-electrode system on an electrochemical workstation (CHI760E). A glassy carbon (GC) electrode (diameter of 5 mm with surface area of 0.196 cm²) was used as a working electrode, while platinum foil was utilized as the counter electrode. The potential was recorded using Ag/AgCl (3.5 M KCl) electrode as the reference electrode. All of the potentials were calibrated to the reversible hydrogen electrode (RHE) according to Nernst equation. To prepare the working electrode, typically, 4 mg of catalyst and 30 μL Nafion solution (Sigma Aldrich, 5 wt %) were dispersed in 1 mL ethanol solution by sonicating for 1 h to form a homogeneous ink. Then 14.7 μL of the dispersion was loaded onto a glassy carbon electrode (loading 0.3 mg/cm²). Before ORR catalytic activity testing, oxygen was used to purge the 0.1 M KOH solution for 30 min to keep the solution oxygen saturation. Before Cyclic voltammetry (CV) and Linear sweep voltammetry (LSV) tests, the working electrodes were activated using CV test at a scan rate of 100 mVs⁻¹ for several times. The linear sweep voltammetry (LSV) were applied at a scan rate of 10 mV s⁻¹. The polarization curves of the ORR was measured from 0.2 to 1.1 V (vs. RHE) at a scan rate of 10 mV s⁻¹ with a series of rotating electrode speeds using a MSR Electrode Rotator (Pine Research Instrumentation). The Pt/C (20 wt% Pt) catalyst which is considered to be one of the best ORR electrocatalysts was used as the reference material, the loading amount of Pt/C was 0.2mg/cm².

Zinc-air battery tests:

A home-made zinc–air battery device was designed for the performance and stability test (Figure. S9). The electrolyte used in the primary zinc-air battery was 6 M KOH. A polished zinc plate was used as the anode and a certain volume of S-600 catalyst ink was brushed onto a 2 cm² carbon

paper (HCP030) as cathode with a catalyst loading of 2 mg cm⁻². As reference materials, 20 wt% Pt/C and Cu/C catalysts were also prepared with the same procedure and loading amount.

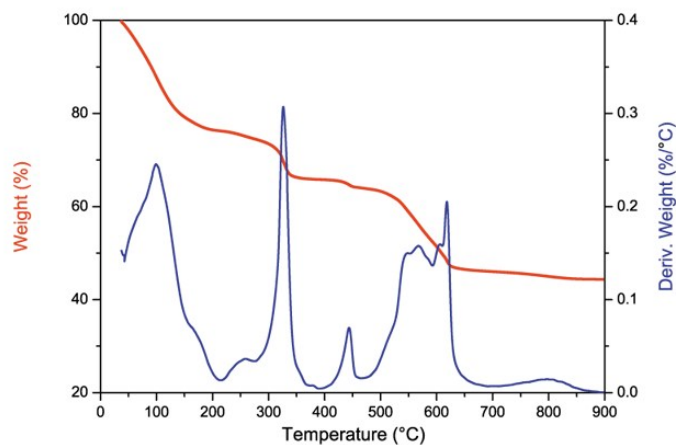


Figure S1. Thermogravimetric analysis (TGA) curves of $\text{Cu}_3[\text{Co}(\text{CN})_6]_2$ under nitrogen atmosphere.

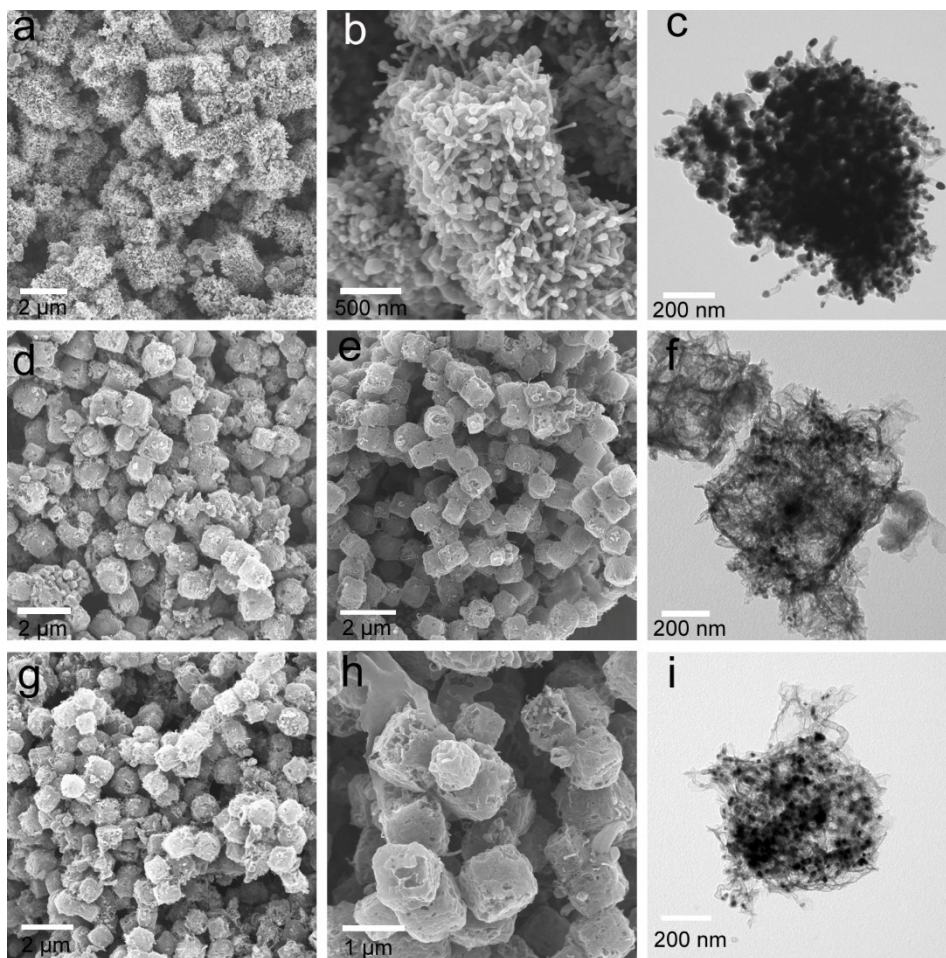


Figure S2. (a,d and g) Field emission scanning electron microscopy (SEM) of Co-600, CuCo-700

and CuCo-800, respectively. (b,e and h) SEM images of Co-600A, S-700 and S-800, respectively. (c,f and i) Transmission electron microscopy (TEM) images of single Co-600A, S-700 and S-800 particles, respectively.

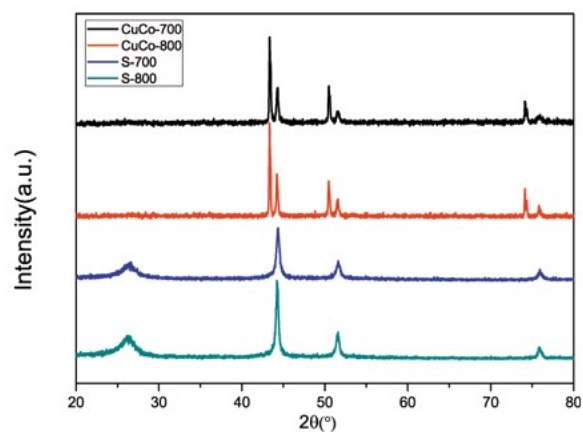


Figure S3. XRD patterns of CuCo-700, CuCo-800, S-700 and S-800.

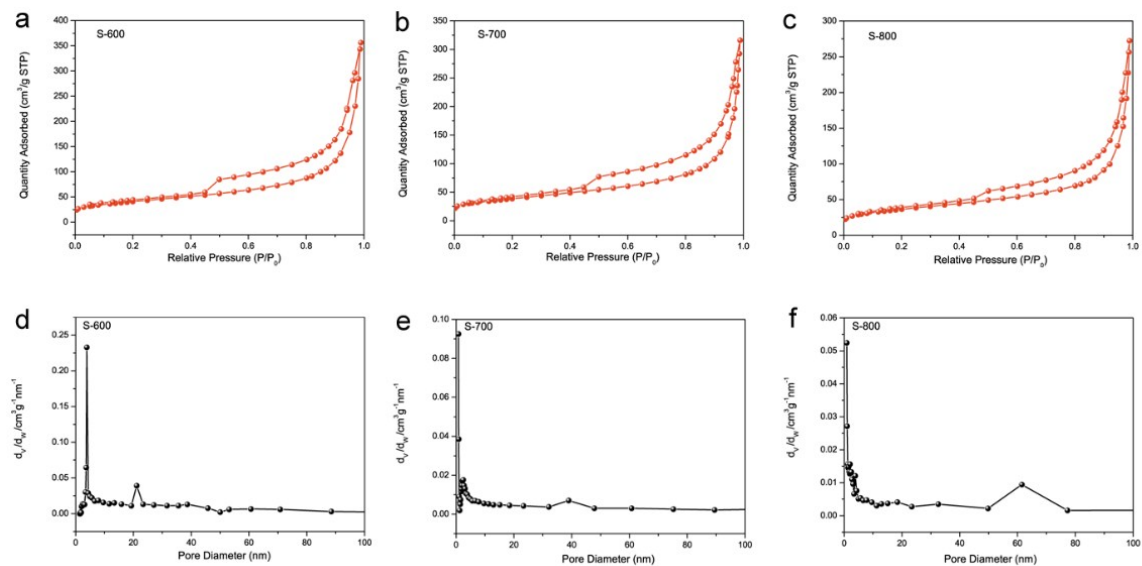


Figure S4. Nitrogen adsorption-desorption isotherm and the corresponding pore size distribution of S-600, S-700, S-800 materials.

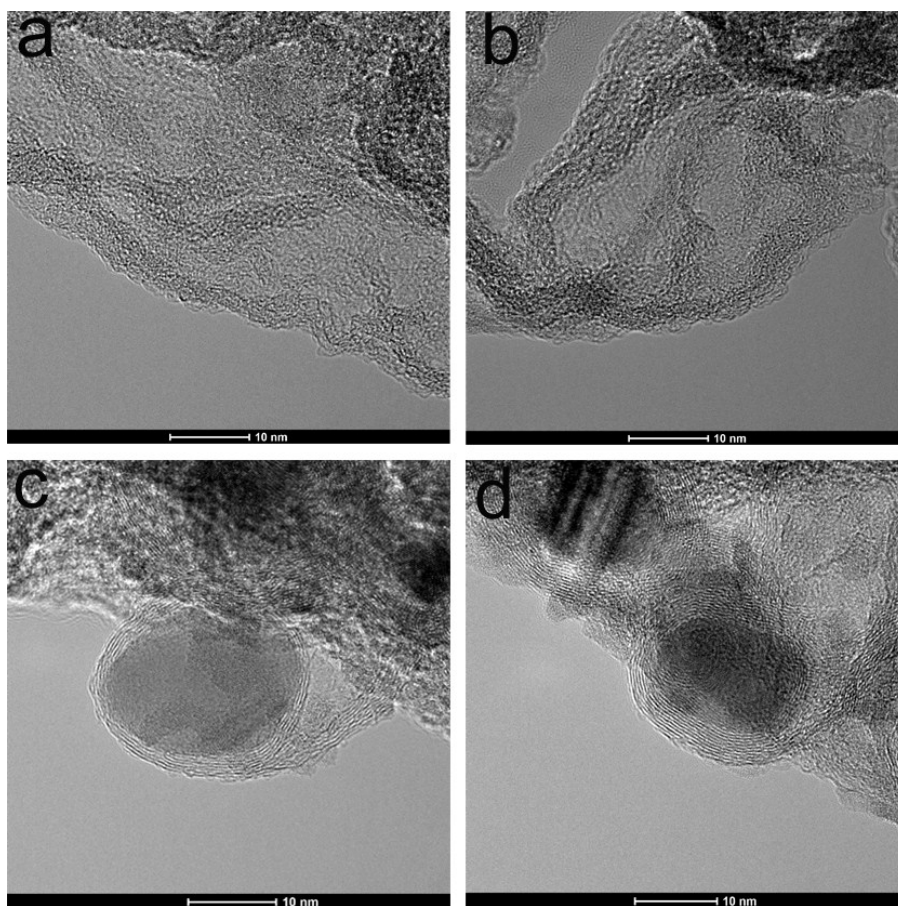


Figure S5. Representative high-resolution transmission electron microscopy images of S-600. (a, b) three dimensional graphene frameworks after etching process. (c, d) some of Co nanoparticles encapsulated by graphene layers are still remained after etching process.

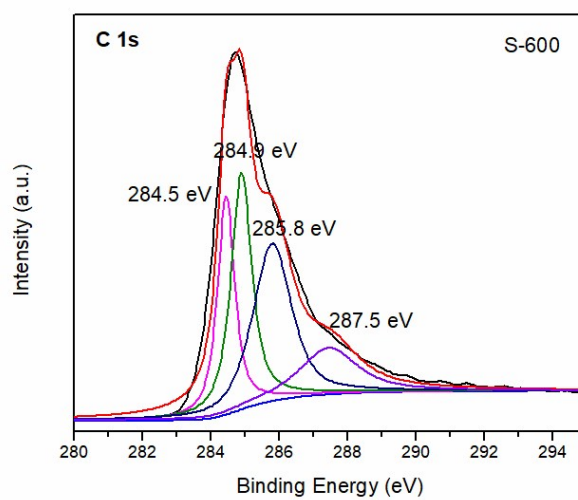


Figure S6. C 1s spectrum of S-600 sample.

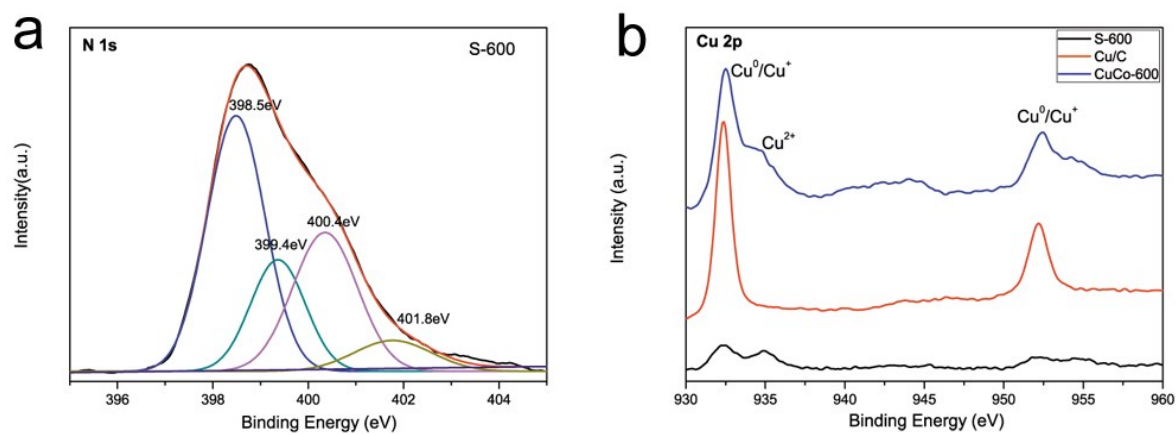


Figure S7. High-resolution XPS spectra of N1s for S-600 and Cu2p for different samples.

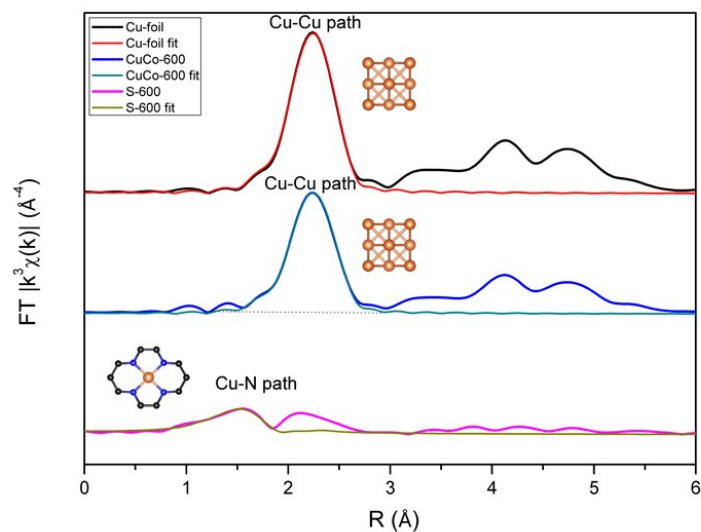


Figure S8. The corresponding EXAFS fitting curves of Cu-foil, CuCo-600 and S-600.

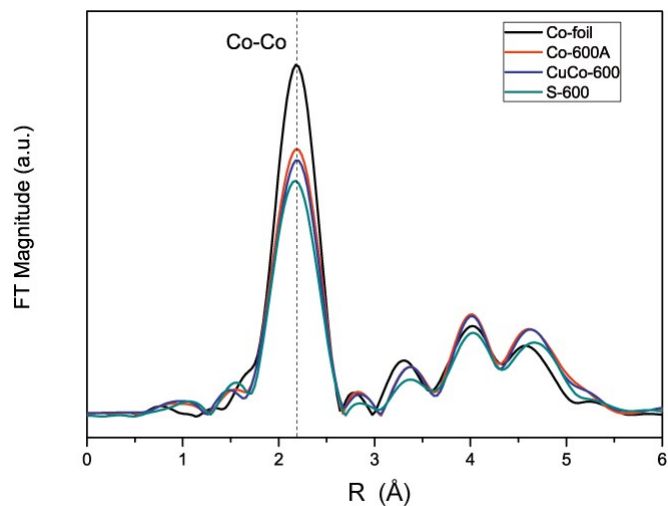


Figure S9. Fourier transform (FT) of the Co K-edge in different samples.

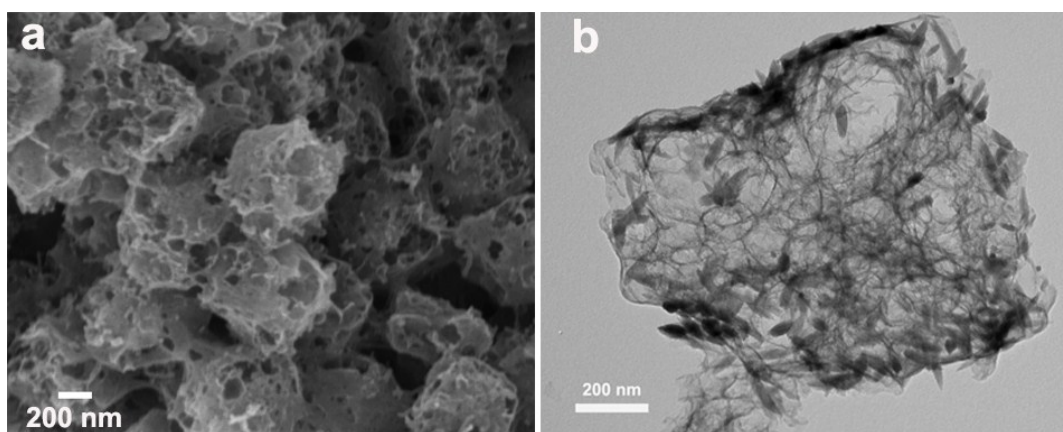


Figure S10. SEM and TEM images of S-600 after 2000th CV cycling.

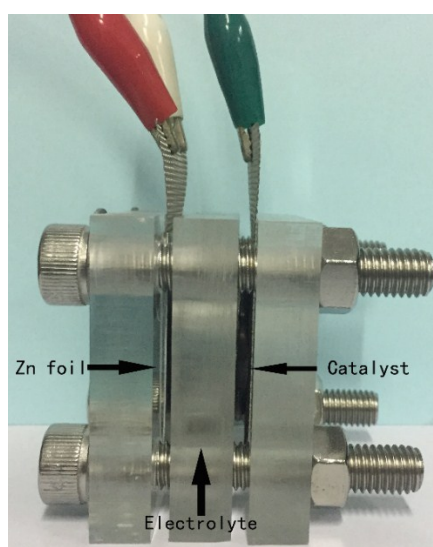


Figure S11. Photograph of homemade zinc-air battery device.

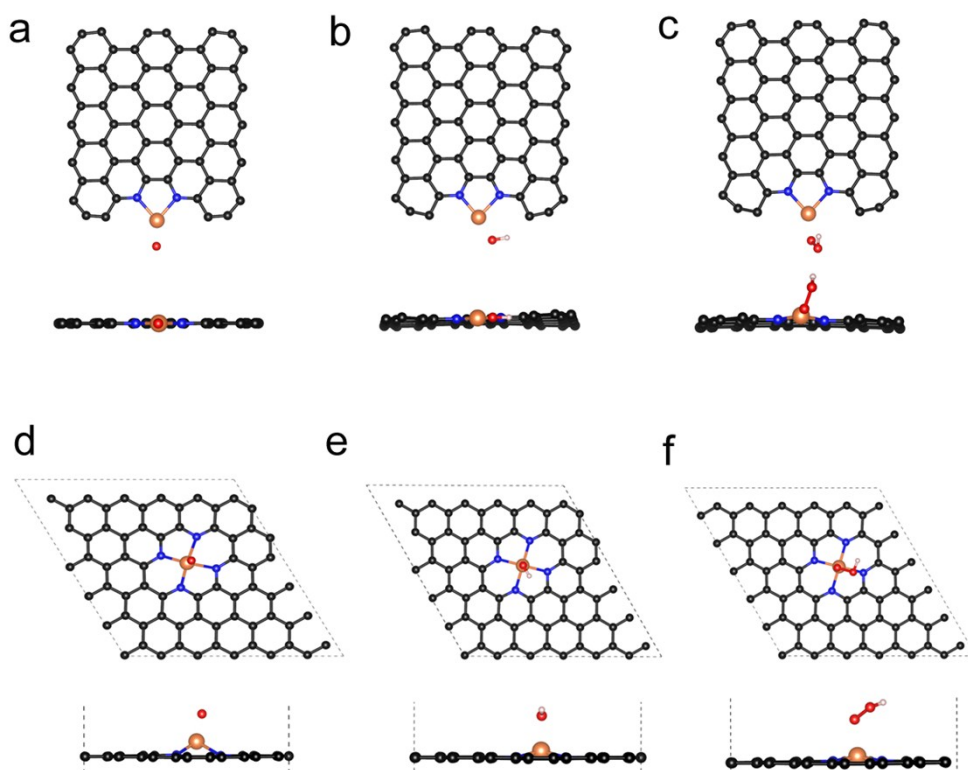


Figure S12. Optimized structures of CuN₂ (a-c) and CuN₄ (d-f) with ORR intermediate states O*, OH* and OOH*. The configurations are illustrated both from top view and side view. Black, blue, orange, red and white balls represent C, N, Cu, O, and H atoms, respectively.

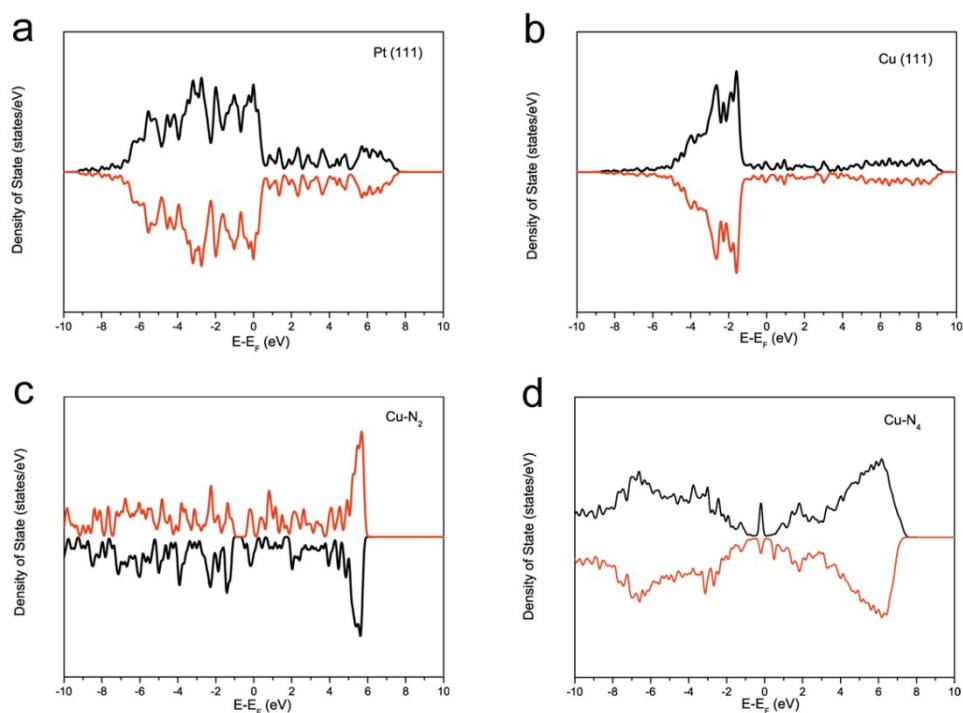


Figure 13. Total density of states (TDOS) of different models: (a) Pt (111) surface model (b) Cu (111) surface model (c) Cu-N₂ model and (d) Cu-N₄ model. The electronic states of both spin-up and spin-down contributions are illustrated.

Sample	CuCo-600	CuCo-700	CuCo-800	S-600	S-700	S-800
Surface Area (m ² g ⁻¹)	41.9	31.3	25.6	176.5	136.8	129.6

Table S1. BET surface of CuCo-600, CuCo-700, CuCo-800 and samples after etching process of S-600, S-700, S-800.

Sample	C (atom%)	N (atom%)	Cu (atom%)	Co (atom%)
S-600	79.05	19.11	0.56	1.28
S-700	86.39	12.86	0.27	0.48
S-800	92.75	6.75	0.18	0.32

Table S2. Chemical compositions of samples after etching process prepared at different annealing temperatures by XPS measurement.

Sample	Path	N	R (Å)	σ^2 (Å ²)	ΔE_0 (eV)
Cu-foil	Cu-Cu	12	2.54 ± 0.002	0.009	3.6
CuCo-600	Cu-Cu	9.4 ± 0.5	2.552 ± 0.003	0.009	4.1
S-600	Cu-N	3.6 ± 0.6	1.974 ± 0.013	0.011	-2.1

Table S3. EXAFS data fitting results of different samples. N is the coordination number; R is distance between absorber and backscatter atoms; σ^2 is the Debye-Waller factor value; E_0 is the inner potential correction to account for the difference in the inner potential between the sample and the reference compound.

Electrocatalysts	Catalyst loading (mg/cm ²)	Onset potential (V vs RHE)	Half-wave potential (V vs RHE)	Reference
S-600	0.3	0.95	0.84	This work
rGO-TADPyCu	0.6	0.95	0.80	Chem. Commun., 2015, 51, 7455
Cu-N/C	0.25	0.91	0.81	Small 2017, 1700740
rGO-Cu_{2-x}S	0.47	0.90	0.82	ACS Catal. 2015, 5, 2534–2540
Cu@N-C	0.6	0.87	0.71	J. Mater. Chem. A, 2015,3, 22031-22034
Co3O4/N-rmGO	0.1	0.88	0.79	Nat. Mater. 2011, 10, 780-786.
NCNTFs	0.2	0.97	0.87	Nat. Energy 2016, 1, 15006.
Fe-N-CNFs	0.6	0.93	0.82	Angew. Chem. Int. Ed. 2015, 54, 8179-8183.
S,N-Fe/N/C-CNT	0.6	Not given	0.85	Angew. Chem. Int. Ed. 2016, 55, 1 – 6
Fe3C@N-CNT	0.25	0.97	0.85	Energy Environ. Sci., 2016, 9, 3092--3096
ZnN_x/BP	0.39	0.99	0.82	Adv. Funct. Mater. 2017, 1700802

Table S4. Comparison of the ORR activity between S-600 with some Cu-based catalyst and other nonprecious ORR catalysts in basic condition (0.1 M KOH) in literatures.

Sample	Cu (wt%)	Co (wt%)
S-600	2.1	11.6
S-700	0.9	10.4
S-800	0.5	10.1

Table S5. The content of Cu and Co obtained from ICP measurements.

Optimized structure	Valence electrons of Cu atom
Cu (111)	11.0
CuN2	10.3
CuN4	10.1

Table.S6. Valence electrons of Cu atom based on Bader charge analysis.